

## Field-free manipulation of exchange bias in perpendicularly magnetized Pt/Co/IrMn structures by spin-orbit torque

Jijun Yun <sup>1</sup>, Qi Zhang,<sup>2</sup> Haiming Xu,<sup>2</sup> Xi Guo,<sup>2</sup> Li Xi <sup>2</sup> and Kexin Jin <sup>1,\*</sup>

<sup>1</sup>*Shaanxi Key Laboratory of Condensed Matter Structures and Properties, and MOE Key Laboratory of Materials Physics and Chemistry under Extraordinary Conditions, School of Physical Science and Technology, Northwestern Polytechnical University, Xi'an 710072, China*

<sup>2</sup>*Key Laboratory for Magnetism and Magnetic Materials of Ministry of Education, and School of Physical Science and Technology, Lanzhou University, Lanzhou 730000, China*



(Received 4 February 2024; accepted 23 May 2024; published 17 June 2024)

Electrical manipulation of exchange bias by spin-orbit torque (SOT) is promising for the design of spintronic devices, such as multilevel memory and neuromorphic computing. However, an external magnetic field is required to assist manipulation of exchange bias, which poses a challenge for applications. In this work, we propose a promising approach to the field-free manipulation of exchange bias through an in-plane ferromagnetic layer deposited on the current line of the Hall bar device, which can generate an internal effective in-plane field to realize field-free SOT switching. Furthermore, our devices present memristive behaviors in the absence of an external field, offering the practical potential for the construction of artificial synapses based on exchange-biased systems. Meanwhile, this method can ensure the high SOT efficiency and a thermal stability factor ( $\Delta$ ) of around 56, indicating over 10 years of data retention. The approach to field-free manipulation of exchange bias by SOT is promising for applications and the development of spintronic devices.

DOI: [10.1103/PhysRevMaterials.8.064407](https://doi.org/10.1103/PhysRevMaterials.8.064407)

### I. INTRODUCTION

Over the past decade, spin-orbit torque (SOT) has emerged as an effective method for manipulating the magnetization of a ferromagnetic (FM) layer in heavy metal (HM)/FM heterostructures [1–5], with potential applications in magnetic memory and spin logic devices [6–9]. In a certain class of antiferromagnets (AFM), SOT has also proved an effective approach to modulating the AFM order [10–13]. For application, AFM materials possess advantages with magnetic field interference immunity and zero stray fields owing to the zero-net magnetization [13,14]. When an AFM layer is in conjunction with a FM layer, an exchange-bias effect can occur, which is usually characterized as a shift of the hysteresis loop along the magnetic field axis [15–17]. From the perspective of application, the exchange-biased system can provide versatile functionalities for spintronic devices and related technologies [13,18].

Recently, SOT was demonstrated to be a promising method to manipulate the exchange bias through switching the FM spins and AFM interfacial spins simultaneously [19–22]. By controlling the magnitude and direction of SOT, the magnetic remanence states can be tailored in exchange-biased HM/FM/AFM systems, which are beneficial to spintronic devices, such as multilevel memory [22,23], neuromorphic computing [21,24], and spin logic [25]. However, an external in-plane magnetic field along the current direction is required to break the symmetry for manipulating exchange

bias or magnetization by SOT in a perpendicularly magnetized HM/FM/AFM system. In order to achieve the field-free SOT-driven magnetization switching, intensive efforts have been made, for example, by introducing a lateral structural asymmetry [26,27], engineering a tilted anisotropy [28,29], using the interlayer exchange coupling [30,31], relying on an inherent magnetocrystalline anisotropy [32], using a magnetic hard mask in the fabrication of SOT-based MRAM [33], and even using an ion-irradiation method [34]. Among those methods, field-free SOT-driven magnetization reversal via exchange bias has been reported widely [31,35,36]. However, field-free manipulation of exchange bias by SOT is rarely reported, which is a challenging issue for the spintronic applications based on exchange-biased systems.

In this work, we propose a promising approach to field-free SOT-induced switching of exchange-bias direction and magnetization in Pt/Co/IrMn systems with perpendicular magnetic anisotropy (PMA). Firstly, Pt/Co/IrMn films were patterned into Hall bar devices, and then a Co(50 nm)/Ta(5 nm) bilayer was capped on both sides of the current channels for the Hall bars to generate an internal in-plane effective field by photolithography and lift-off techniques. The magnetotransport measurements demonstrate the field-free manipulation of exchange bias and magnetization by SOT. Furthermore, stable multilevel remanent Hall resistances can be field-free tailored by successive current pulses, analogous to synaptic plasticity, with potential applications in neuromorphic systems. Finally, the thermal stability of the device is investigated. The thermal stability factor  $\Delta$  is around 56, indicating that the device can maintain data nonvolatility for over 10 years [37]. The method of field-free manipulating exchange bias

\*Contact author: [jinkx@nwpu.edu.cn](mailto:jinkx@nwpu.edu.cn)

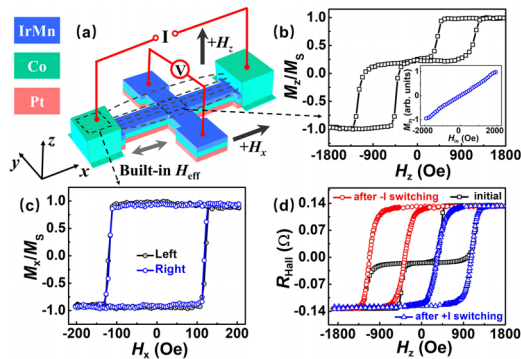


FIG. 1. (a) Device structure with schematic of the magneto-transport measurements. (b) Polar MOKE hysteresis loop for the Hall cross of the device under the out-of-plane magnetic field  $H_z$ . The inset shows the dependence of in-plane magnetization  $M_{in}$  on in-plane magnetic field  $H_{in}$ . (c) The in-plane hysteresis loops for Co(50 nm) covering layer of the device by MOKE. (d) Anomalous Hall hysteresis loops for the Hall cross in the as-deposited state (black), after positive (blue), and negative (red) current switching with an amplitude of  $5.06 \times 10^6$  A/cm<sup>2</sup> subject to an in-plane field  $H_x = +500$  Oe.

by SOT would be promising for potential applications based on exchange-biased systems, such as multilevel storage and artificial synapses.

## II. EXPERIMENTAL METHODS

The film stacks Ta(3)/Pt(5)/Co(0.8)/Ir<sub>20</sub>Mn<sub>80</sub>(6)/Ta(2.5) (thickness in nm) were deposited on Corning glass substrates by direct current magnetron sputtering with a base pressure below  $5.0 \times 10^{-5}$  Pa. The films were then patterned into 20  $\mu$ m wide Hall bars using standard lithography and argon ion milling techniques. A Co(50 nm)/Ta(5 nm) bilayer was capped on both sides of the current channels for the Hall bars by photolithography and lift-off techniques. Particularly, the Co/Ta bilayer was deposited with an *in situ* in-plane magnetic field (500 Oe) along the current channel to ensure the in-plane magnetic anisotropy of Co(50 nm).

The characterization of the hysteresis loops for the as-deposited samples was carried out through magnetic-optical Kerr effect (MOKE) microscopy measurements. The anomalous Hall resistance measurements were carried out using a Keithley 6221 as the current source. For each Hall resistance, a constant 0.1 mA bias current was applied to read the Hall voltage. Additionally, the magnetic domain images of the Hall bars were observed using a MOKE microscope operating on a differential model.

## III. RESULTS AND DISCUSSION

### A. Field-free manipulation of exchange bias

As sketched in Fig. 1(a), the in-plane Co bars are expected to generate a built-in effective in-plane magnetic field  $H_{eff}$ , parallel to the current channel of the Hall bar. Figure 1(b) shows the typical double-biased hysteresis loop, resulting from the coexistence of up- and down-magnetized Co subdomains with opposite exchange-bias fields ( $H_{ex}$ ). The

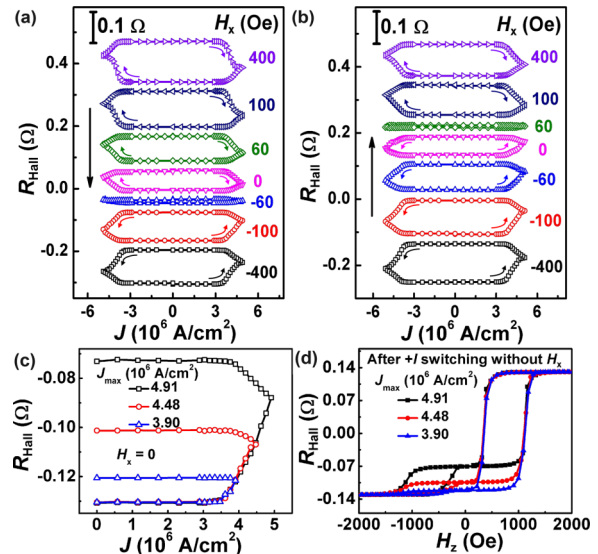


FIG. 2. (a,b) Current-induced magnetization switching loops under different in-plane fields  $H_x$  varying from 400 to  $-400$  Oe (a), and  $-400$  to 400 Oe (b). Black arrows indicate the sequence of applied in-plane fields. (c) Anomalous Hall resistance versus current density with varying magnitudes of maximal current density ( $J_{max}$ ) under  $H_x = 0$ . (d) Hysteresis loops after positive-current-induced SOT switching with different  $J_{max}$  under  $H_x = 0$ .

perpendicular hysteresis loop and in-plane linear magnetization response to the magnetic field demonstrate the PMA of the Pt/Co/IrMn sample. Based on the Stoner-Wohlfarth model, the PMA effective field is determined to be  $9190 \pm 20$  Oe (for details see the Supplemental Material [38]). As shown in Fig. 1(c), we also measured the hysteresis loops of the Co(50 nm) layer, which confirms that the Co(50 nm) layer possesses in-plane magnetic anisotropy.

Afterwards, the magnetotransport measurements were performed. To evaluate the SOT quantitatively, the harmonic Hall voltage measurement technique was employed (for details see the Supplemental Material [38]). The SOT efficiency, expressed as the dampinglike effective field per unit current density, is determined to be  $5.82$  Oe/( $10^6$  A/cm<sup>2</sup>), which aligns with previous reports [19,43]. Based on anomalous Hall measurement, we investigated the SOT-induced switching of exchange bias and magnetization. The SOT switching was performed by sweeping positive/negative current pulses with a pulse width of 1 ms subject to a fixed  $H_x = +500$  Oe. Figure 1(d) shows the hysteresis loop in the as-deposited state, which evolves to a positive/negative-biased loop following the application of positive/negative current pulses. The maximal magnitude of applied current density ( $J_{max}$ ) is  $5.06 \times 10^6$  A/cm<sup>2</sup>, and the generated SOT is large enough to tune the  $H_{ex}$  between positive and negative values in Pt/Co/IrMn trilayers with a single-biased hysteresis loop. This result confirms that SOT can effectively switch the direction of exchange bias in the Pt/Co/IrMn system, aligning with previous reports [19–22].

Figures 2(a) and 2(b) illustrate the current-induced magnetization switching loops under different in-plane fields  $H_x$  varying from 400 to  $-400$  Oe, and  $-400$  to 400 Oe,

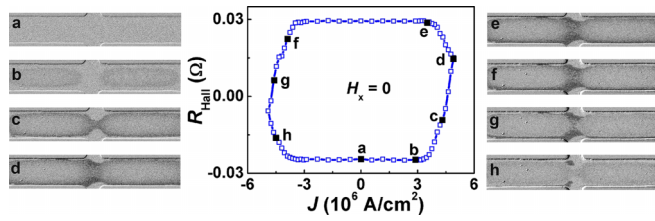


FIG. 3. Field-free current-induced magnetization switching loops and corresponding magnetic domain images.

respectively. The switching chirality is clockwise/counterclockwise when  $H_x$  is positive/negative, consistent with the positive effective spin Hall angle of our Pt/Co/IrMn sample. Moreover, the field-free magnetization switching can be achieved. When  $H_x$  varies from 400 to  $-400$  Oe, the magnetization switching is not observed at  $H_x = -60$  Oe. The phenomena can be attributed to the built-in effective magnetic field  $H_{\text{eff}}$  of approximately 60 Oe, generated by the two Co bars, facilitating the field-free SOT switching. When  $H_x$  changes from  $-400$  to 400 Oe, the switching chirality of the loops is reversed at  $H_x = +60$  Oe, confirming that the magnitude of  $H_{\text{eff}}$  in such a device is around 60 Oe. Subsequently, we focus on the field-free SOT switching. By changing the  $J_{\text{max}}$ , the anomalous Hall resistance  $R_{\text{Hall}}$  is switched to different values, as depicted in Fig. 2(c). For comparison, the  $R_{\text{Hall}}$  is set to  $-0.13 \Omega$  initially by applying a current pulse of  $J = -5.06 \times 10^6 \text{ A/cm}^2$  and  $H_x = -500$  Oe. After each current-induced SOT switching, the hysteresis loops are measured and are summarized in Fig. 2(d). Clearly, the remanent state changes after each SOT switching, while the magnitude of  $H_{\text{ex}}$  remains constant at approximately 740 Oe. These results confirm that field-free tuning magnetization and exchange bias by SOT can change the remanence state in HM/FM/AFM systems, which holds promise for applications due to the relatively stable multilevel storage states. It should be noted that the field-free SOT switching is only partial, mainly because the effective in-plane field produced by Ta/Co is not large enough to achieve full switching. For complete application, further experiments are required. For instance, employing a FM layer with larger magnetic anisotropy as a “permanent magnet” to provide a stronger built-in bias field, or decreasing the PMA of the exchange-biased system to lower the threshold for switching, may be effective approaches.

To gain insight into the magnetization dynamics associated with the change in  $R_{\text{Hall}}$ , the domain images were recorded by the MOKE microscope operating on a differential model [44]. Figure 3 shows the field-free SOT-induced magnetization switching loop and corresponding magnetic domains images. Starting from a down-magnetized state, the application of successive positive current pulses nucleates reversed domains at the current line. These domains grow progressively, accompanied by continuous variation of  $R_{\text{Hall}}$ . When the current polarity is reversed and  $J$  reaches a critical value, the reversed domains shrink gradually upon the application of successive negative current pulses. The unique behavior of domain wall motion in the Hall cross can be explained by the nonuniform distribution of current density in the Hall cross [21,31]. Additionally, the irregular shape of the domain wall (tilting

of domain wall) outside the Hall cross may be ascribed to complicated mechanisms, such as the Dyzaloshinskii–Moriya interaction (DMI) [45], edge effect of the sample [46], domain wall speed asymmetry [47], and Oersted field [48], which needs further experimental investigation. Moreover, MOKE images indicate the absence of switching along the current line, potentially due to a low built-in field from the Co/Ta and a large DMI field in the domain wall. Our analysis suggests that the built-in field from the Co/Ta ( $\sim 60$  Oe) is weaker than the effective DMI field at the Pt/Co interface, which ranges from hundreds to thousands of oersteds [4,49]. Consequently, this discrepancy in field strength is likely insufficient to completely bias the chirality of the Néel domain walls necessary for effective switching. Nonetheless, these MOKE images intuitively demonstrate that the field-free switching in our Pt/Co/IrMn system results from domain wall motion.

### B. Mimicking synaptic behaviors

One of the most important applications of memristive behavior is artificial synapses, which are indispensable building blocks in neuromorphic computing [50–53]. A synapse is a conjunction between two neuron cells, termed a preneuron and a postneuron [54,55]. When a preneuron is excited, it releases the neurotransmitters that are transmitted across the synapse to the postneuron, resulting in either an excitatory postsynaptic potential (EPSP) or an inhibitory postsynaptic potential (IPSP), along with updates to synaptic weight [56,57]. The synaptic weight represents the strength of the correlation between two neighboring neurons. Information storage and learning in the human brain are exactly a result of changes in synaptic weight. Synaptic plasticity refers to the ability of synapses to dynamically adjust synaptic weights. Typically, the synaptic behaviors can be mimicked by the responses of resistance changes to the programming of successive current pulses [50–53].

As sketched in Fig. 4(a), an artificial synapse based on the Pt/Co/IrMn structure can be achieved by regarding the  $R_{\text{Hall}}$  as the synaptic weight, which can be modulated by the applied current pulses. As illustrated in Fig. 4(b), as the number of positive/negative current pulses increases, the  $R_{\text{Hall}}$  increases/decreases gradually, emulating the synaptic plasticity of EPSP/IPSP, respectively. Initially, the magnetization was set into the up state by a positive reset current pulse ( $J \approx 5.06 \times 10^6 \text{ A/cm}^2$ ) under  $H_x = -500$  Oe. Subsequently, a series of 100 current pulses, with an amplitude of  $4.91 \times 10^6 \text{ A/cm}^2$  and a pulse width of 0.2 ms, was applied with negative polarity (black points) and positive polarity (red points). The response of  $R_{\text{Hall}}$  to current pulses can be utilized to simulate synaptic plasticity behaviors. Particularly, the  $R_{\text{Hall}}$  of Pt/Co/IrMn stacks is the remanent state and quite stable over time, classifying the EPSP and IPSP here as long-term plasticity [50,57].

### C. Thermal stability of the devices

From the perspective of practical applications, the thermal stability factor  $\Delta$  is a critical parameter as it determines the service life of a recording bit for data storage [37,58]. The  $\Delta$  is defined as  $E_B/k_B T$  with  $E_B$  the activation energy barrier,

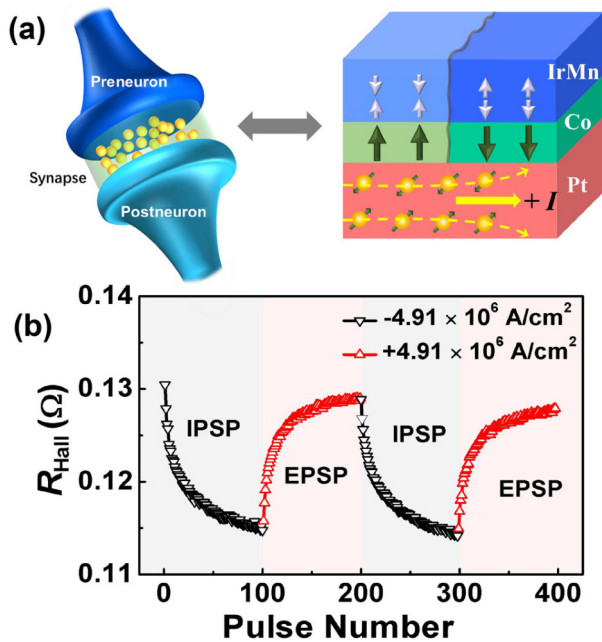


FIG. 4. (a) Left: the schematic of a synapse sandwiched between pre- and postneurons. Right: the sketch of the Pt/Co/IrMn system to realize synapse function. The light-colored area shows the up-magnetized domain, while the dark-colored area shows the down-magnetized domain. (b)  $R_{\text{Hall}}$  responses to successive current pulses with negative polarity (black points) and positive polarity (red points) with current density of  $4.91 \times 10^6 \text{ A/cm}^2$  and fixed pulse width of 0.2 ms.

$k_B$  the Boltzmann constant, and  $T$  the absolute temperature. Since the magnetization switching is a thermally activated process, the coercive field  $H_C$  is expected to depend on the magnetic field sweeping rate. As demonstrated in Fig. 5(a), the switching event occurs at lower fields with slower sweeping rates. Here, the sweeping rate ranges from 1 to 100 Oe/s. The dependence of  $H_C$  on sweeping rate can be expressed as [59,60]

$$H_C = H_k \left[ 1 - \sqrt{\frac{1}{\Delta} \ln \left( \frac{f_0 H_k}{2\Delta R} \right)} \right], \quad (1)$$

where  $R = dH/dt$  is the field sweeping rate,  $H_k$  is the anisotropy field, and  $f_0$  is an attempt frequency

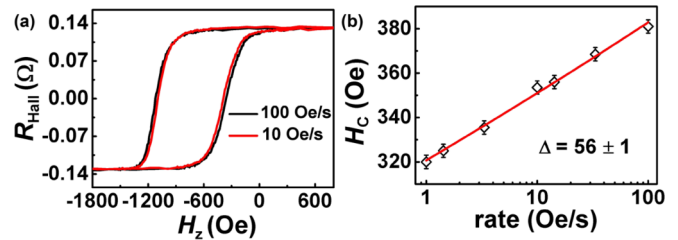


FIG. 5. (a) Typical magnetic hysteresis loops of the sample with the variation of magnetic field sweeping rate of 10 and 100 Oe/s. (b) The sweeping-rate-dependent coercive field  $H_C$ .

( $f_0 = 1 \times 10^{10} \text{ Hz}$ ). Figure 5(b) shows that Eq. (1) (solid lines) fits the experimental data well and  $\Delta$  is around 56. This value means that it can ensure the nonvolatility for the data storage over 10 years [37]. Besides,  $\Delta$  for this sample is almost the same as that for the reference device (Pt/Co/IrMn device without in-plane Co layer on current line; see the Supplemental Material [38]). This similarity indicates that our method can realize field-free switching of exchange-bias direction and ensure the thermal stability in the meantime.

#### IV. CONCLUSION

In summary, we propose a promising approach to manipulating exchange bias by SOT without the assistance of an external magnetic field. This method involves the deposition of an in-plane FM layer directly on the current line of a Hall bar device, which generates an internal effective in-plane field, enabling field-free SOT switching. Moreover, this approach does not compromise the thermal stability of the device, and its  $\Delta$  is around 56, showing the potential for over 10 years of data retention time. Further, the memristive behavior in the Pt/Co/IrMn system can be utilized to simulate a synaptic behavior of EPSP/IPSP. This work provides an effective means for field-free manipulation of exchange bias via SOT, which shows promise for applications in multilevel storage and artificial synapses.

#### ACKNOWLEDGMENTS

This work is supported by the National Natural Science Foundation of China (Grants No. 51671098, No. 52373253, and No. 12374192), the 111 Project (Grant No. B20063), the Natural Science Foundation of Gansu Province (Grant No. 22JR5RA474), the Fundamental Research Funds for the Central Universities (Grant No. 5000220455), and the Natural Science Basic Research Program of Shaanxi (Program No. 2024JC-YBQN-0374).

[1] L. Liu, C.-F. Pai, Y. Li, H. W. Tseng, D. C. Ralph, and R. A. Buhrman, Spin-torque switching with the giant spin Hall effect of tantalum, *Science* **336**, 555 (2012).  
 [2] I. M. Miron, K. Garello, G. Gaudin, P.-J. Zermatten, M. V. Costache, S. Auffret, S. Bandiera, B. Rodmacq, A. Schuhl, and P. Gambardella, Perpendicular switching of a single ferromagnetic layer induced by in-plane current injection, *Nature (London)* **476**, 189 (2011).

[3] S. Woo, M. Mann, A. J. Tan, L. Caretta, and G. S. D. Beach, Enhanced spin-orbit torques in Pt/Co/Ta heterostructures, *Appl. Phys. Lett.* **105**, 212404 (2014).  
 [4] J. Yun, Y. Zuo, J. Mao, M. Chang, S. Zhang, J. Liu, and L. Xi, Lowering critical current density for spin-orbit torque induced magnetization switching by ion irradiation, *Appl. Phys. Lett.* **115**, 032404 (2019).  
 [5] X. Han, X. Wang, C. Wan, G. Yu, and X. Lv, Spin-orbit torques:

- Materials, physics, and devices, *Appl. Phys. Lett.* **118**, 120502 (2021).
- [6] R. Ramaswamy, J. M. Lee, K. Cai, and H. Yang, Recent advances in spin-orbit torques: Moving towards device applications, *Appl. Phys. Rev.* **5**, 031107 (2018).
- [7] Y. Cao, G. Xing, H. Lin, N. Zhang, H. Zheng, and K. Wang, Prospect of spin-orbitronic devices and their applications, *iScience* **23**, 101614 (2020).
- [8] Y. Li, K. W. Edmonds, X. Liu, H. Zheng, and K. Wang, Manipulation of magnetization by spin-orbit torque, *Adv. Quantum Technol.* **2**, 1800052 (2019).
- [9] C. Song, R. Zhang, L. Liao, Y. Zhou, X. Zhou, R. Chen, Y. You, X. Chen, and F. Pan, Spin-orbit torques: Materials, mechanisms, performances, and potential applications, *Prog. Mater. Sci.* **118**, 100761 (2021).
- [10] P. Wadley, B. Howells, J. Železný, C. Andrews, V. Hills, R. P. Campion, V. Novák, K. Olejník, F. Maccherozzi, S. S. Dhesi, S. Y. Martin, T. Wagner, J. Wunderlich, F. Freimuth, Y. Mokrousov, J. Kuneš, J. S. Chauhan, M. J. Grzybowski, A. W. Rushforth, K. W. Edmonds *et al.*, Electrical switching of an antiferromagnet, *Science* **351**, 587 (2016).
- [11] J. Železný, H. Gao, A. Manchon, F. Freimuth, Y. Mokrousov, J. Zemen, J. Mašek, J. Sinova, and T. Jungwirth, Spin-orbit torques in locally and globally noncentrosymmetric crystals: Antiferromagnets and ferromagnets, *Phys. Rev. B* **95**, 014403 (2017).
- [12] S. Yu. Bodnar, L. Šmejkal, I. Turek, T. Jungwirth, O. Gomonay, J. Sinova, A. A. Sapozhnik, H.-J. Elmers, M. Kläui, and M. Jourdan, Writing and reading antiferromagnetic Mn<sub>2</sub>Au by Néel spin-orbit torques and large anisotropic magnetoresistance, *Nat. Commun.* **9**, 348 (2018).
- [13] J. Železný, P. Wadley, K. Olejník, A. Hoffmann, and H. Ohno, Spin transport and spin torque in antiferromagnetic devices, *Nat. Phys.* **14**, 220 (2018).
- [14] T. Jungwirth, X. Marti, P. Wadley, and J. Wunderlich, Antiferromagnetic spintronics, *Nat. Nanotechnol.* **11**, 231 (2016).
- [15] J. Nogués and I. K. Schuller, Exchange bias, *J. Magn. Magn. Mater.* **192**, 203 (1999).
- [16] O. Petravic, Z.-P. Li, I. V. Roshchin, M. Viret, R. Morales, X. Batlle, and I. K. Schuller, Bidomain state in exchange biased FeF<sub>2</sub>/Ni, *Appl. Phys. Lett.* **87**, 222509 (2005).
- [17] S. Brück, J. Sort, V. Baltz, S. Suriñach, J. S. Muñoz, B. Dieny, M. D. Baró, and J. Nogués, Exploiting length scales of exchange-bias systems to fully tailor double-shifted hysteresis loops, *Adv. Mater.* **17**, 2978 (2005).
- [18] D. Xiong, Y. Jiang, K. Shi, A. Du, Y. Yao, Z. Guo, D. Zhu, K. Cao, S. Peng, W. Cai, D. Zhu, and W. Zhao, Antiferromagnetic spintronics: An overview and outlook, *Fundam. Res.* **2**, 522 (2022).
- [19] P.-H. Lin, B.-Y. Yang, M.-H. Tsai, P.-C. Chen, K.-F. Huang, H.-H. Lin, and C.-H. Lai, Manipulating exchange bias by spin-orbit torque, *Nat. Mater.* **18**, 335 (2019).
- [20] S. Peng, D. Zhu, W. Li, H. Wu, A. J. Grutter, D. A. Gilbert, J. Lu, D. Xiong, W. Cai, P. Shafer, K. L. Wang, and W. Zhao, Exchange bias switching in an antiferromagnet/ferromagnet bilayer driven by spin-orbit torque, *Nat. Electron.* **3**, 757 (2020).
- [21] J. Yun, Q. Bai, Z. Yan, M. Chang, J. Mao, Y. Zuo, D. Yang, L. Xi, and D. Xue, Tailoring multilevel-stable remanence states in exchange-biased system through spin-orbit torque, *Adv. Funct. Mater.* **30**, 1909092 (2020).
- [22] X. H. Liu, K. W. Edmonds, Z. P. Zhou, and K. Y. Wang, Tuning interfacial spins in antiferromagnetic-ferromagnetic-heavy-metal heterostructures via spin-orbit torque, *Phys. Rev. Appl.* **13**, 014059 (2020).
- [23] Z. Yan, J. J. Yun, W. B. Sui, L. Xi, Z. T. Xie, J. W. Cao, M. S. Si, D. Z. Yang, and D. S. Xue, Current switching of interface antiferromagnet in ferromagnet/antiferromagnet heterostructure, *Appl. Phys. Lett.* **118**, 032402 (2021).
- [24] J. Kang, J. Ryu, J.-G. Choi, T. Lee, J. Park, S. Lee, H. Jang, Y. S. Jung, K.-J. Kim, and B.-G. Park, Current-induced manipulation of exchange bias in IrMn/NiFe bilayer structures, *Nat. Commun.* **12**, 6420 (2021).
- [25] Y. Fan, X. Han, X. Zhao, Y. Dong, Y. Chen, L. Bai, S. Yan, and Y. Tian, Programmable spin-orbit torque multistate memory and spin logic cell, *ACS Nano* **16**, 6878 (2022).
- [26] G. Yu, P. Upadhyaya, Y. Fan, J. G. Alzate, W. Jiang, K. L. Wong, S. Takei, S. A. Bender, L.-T. Chang, Y. Jiang, M. Lang, J. Tang, Y. Wang, Y. Tserkovnyak, P. K. Amiri, and K. L. Wang, Switching of perpendicular magnetization by spin-orbit torques in the absence of external magnetic fields, *Nat. Nanotechnol.* **9**, 548 (2014).
- [27] B. Cui, H. Wu, D. Li, S. A. Razavi, D. Wu, K. L. Wong, M. Chang, M. Gao, Y. Zuo, L. Xi, and K. L. Wang, Field-free spin-orbit torque switching of perpendicular magnetization by the Rashba interface, *ACS Appl. Mater. Interfaces* **11**, 39369 (2019).
- [28] L. You, O. J. Lee, D. Bhowmik, D. Labanowski, J. Hong, J. Bokor, and S. Salahuddin, Switching of perpendicularly polarized nanomagnets with spin orbit torque without an external magnetic field by engineering a tilted anisotropy, *Proc. Natl. Acad. Sci. USA* **112**, 10310 (2015).
- [29] M. Chang, J. Yun, Y. Zhai, B. Cui, Y. Zuo, G. Yu, and L. Xi, Field free magnetization switching in perpendicularly magnetized Pt/Co/FeNi/Ta structure by spin orbit torque, *Appl. Phys. Lett.* **117**, 142404 (2020).
- [30] Y.-C. Lau, D. Betto, K. Rode, J. M. D. Coey, and P. Stamenov, Spin-orbit torque switching without an external field using interlayer exchange coupling, *Nat. Nanotechnol.* **11**, 758 (2016).
- [31] A. van den Brink, G. Vermeij, A. Solignac, J. Koo, J. T. Kohlhepp, H. J. M. Swagten, and B. Koopmans, Field-free magnetization reversal by spin-Hall effect and exchange bias, *Nat. Commun.* **7**, 10854 (2016).
- [32] L. Liu, Q. Qin, W. Lin, C. Li, Q. Xie, S. He, X. Shu, C. Zhou, Z. Lim, J. Yu, W. Lu, M. Li, X. Yan, S. J. Pennycook, and J. Chen, Current-induced magnetization switching in all-oxide heterostructures, *Nat. Nanotechnol.* **14**, 939 (2019).
- [33] K. Garello, F. Yasin, H. Hody, S. Couet, L. Souriau, S. H. Sharifi, J. Swerts, R. Carpenter, S. Rao, W. Kim, J. Wu, K. K. V. Sethu, M. Pak, N. Jossart, D. Crotti, A. Furnémont, and G. S. Kar, Manufacturable 300mm platform solution for field-free switching SOT-MRAM, in *2019 Symposium on VLSI Technology, Kyoto, Japan* (IEEE, Piscataway, NJ, 2019), pp. T194-T195.
- [34] X. He, Y. Sheng, J. Yun, J. Zhang, H. Xie, Y. Ren, B. Cui, Y. Zuo, and L. Xi, Ion-irradiation-induced field-free magnetization switching in synthetic antiferromagnets by spin-orbit torque, *J. Magn. Magn. Mater.* **582**, 170977 (2023).

- [35] Y.-W. Oh, S.-h. C. Baek, Y. M. Kim, H. Y. Lee, K.-D. Lee, C.-G. Yang, E.-S. Park, K.-S. Lee, K.-W. Kim, G. Go, J.-R. Jeong, B.-C. Min, H.-W. Lee, K.-J. Lee, and B.-G. Park, Field-free switching of perpendicular magnetization through spin-orbit torque in antiferromagnet/ferromagnet/oxide structures, *Nat. Nanotechnol.* **11**, 878 (2016).
- [36] W. J. Kong, Y. R. Ji, X. Zhang, H. Wu, Q. T. Zhang, Z. H. Yuan, C. H. Wan, X. F. Han, T. Yu, K. Fukuda, H. Naganuma, and M.-J. Tung, Field-free spin Hall effect driven magnetization switching in Pd/Co/IrMn exchange coupling system, *Appl. Phys. Lett.* **109**, 132402 (2016).
- [37] L. Thomas, G. Jan, S. Le, and P.-K. Wang, Quantifying data retention of perpendicular spin-transfer-torque magnetic random access memory chips using an effective thermal stability factor method, *Appl. Phys. Lett.* **106**, 162402 (2015).
- [38] See Supplemental Material at <http://link.aps.org/supplemental/10.1103/PhysRevMaterials.8.064407> for the measurements of effective PMA field, SOT efficiency, and thermal stability of reference device, which includes Refs. [39–42].
- [39] S. Emori, U. Bauer, S. Woo, and G. S. D. Beach, Large voltage-induced modification of spin-orbit torques in Pt/Co/GdOx, *Appl. Phys. Lett.* **105**, 222401 (2014).
- [40] D. Li, S. Chen, Y. Zuo, J. Yun, B. Cui, K. Wu, X. Guo, D. Yang, J. Wang, and L. Xi, Roles of Joule heating and spin-orbit torques in the direct current induced magnetization reversal, *Sci. Rep.* **8**, 12959 (2018).
- [41] J. Kim, J. Sinha, M. Hayashi, M. Yamanouchi, S. Fukami, T. Suzuki, S. Mitani, and H. Ohno, Layer thickness dependence of the current-induced effective field vector in Ta|CoFeB|MgO, *Nat. Mater.* **12**, 240 (2013).
- [42] R. Takemura, T. Kawahara, K. Miura, H. Yamamoto, J. Hayakawa, N. Matsuzaki, K. Ono, M. Yamanouchi, K. Ito, H. Takahashi, S. Ikeda, H. Hasegawa, H. Matsuoka, and H. Ohno, A 32-Mb SPRAM with 2T1R memory cell, localized bi-directional write driver and '1'/0' dual-array equalized reference scheme, *IEEE J. Solid-State Circuits* **45**, 869 (2010).
- [43] X. Guo, J. Yun, Q. Bai, Y. Zuo, and L. Xi, Enhancement of writing efficiency for multilevel memory in perpendicularly magnetized Pt/Co/Pt/IrMn multilayers, *J. Magn. Magn. Mater.* **564**, 170111 (2022).
- [44] B. Cui, D. Li, J. Yun, Y. Zuo, X. Guo, K. Wu, X. Zhang, Y. Wang, L. Xi, and D. Xue, Magnetization switching through domain wall motion in Pt/Co/Cr racetracks with the assistance of the accompanying Joule heating effect, *Phys. Chem. Chem. Phys.* **20**, 9904 (2018).
- [45] O. Boulle, S. Rohart, L. D. Buda-Prejbeanu, E. Jué, I. M. Miron, S. Pizzini, J. Vogel, G. Gaudin, and A. Thiaville, Domain wall tilting in the presence of the Dzyaloshinskii-Moriya interaction in out-of-plane magnetized magnetic nanotracks, *Phys. Rev. Lett.* **111**, 217203 (2013).
- [46] S. Pizzini, J. Vogel, S. Rohart, L. D. Buda-Prejbeanu, E. Jué, O. Boulle, I. M. Miron, C. K. Safeer, S. Auffret, G. Gaudin, and A. Thiaville, Chirality-induced asymmetric magnetic nucleation in Pt/Co/AlO<sub>x</sub> ultrathin microstructures, *Phys. Rev. Lett.* **113**, 047203 (2014).
- [47] D.-Y. Kim, M.-H. Park, Y.-K. Park, J.-S. Kim, Y.-S. Nam, H.-S. Hwang, D.-H. Kim, S.-G. Je, B.-C. Min, and S.-B. Choe, Magnetic domain-wall tilting due to domain-wall speed asymmetry, *Phys. Rev. B* **97**, 134407 (2018).
- [48] D. Li, B. Cui, J. Yun, M. Chen, X. Guo, K. Wu, X. Zhang, Y. Wang, J. Mao, Y. Zuo, J. Wang, and L. Xi, Current-induced domain wall motion and tilting in perpendicularly magnetized racetracks, *Nanoscale Res. Lett.* **13**, 238 (2018).
- [49] C.-F. Pai, M. Mann, A. J. Tan, and G. S. D. Beach, Determination of spin torque efficiencies in heterostructures with perpendicular magnetic anisotropy, *Phys. Rev. B* **93**, 144409 (2016).
- [50] S. Zhang, S. Luo, N. Xu, Q. Zou, M. Song, J. Yun, Q. Luo, Z. Guo, R. Li, W. Tian, X. Li, H. Zhou, H. Chen, Y. Zhang, X. Yang, W. Jiang, K. Shen, J. Hong, Z. Yuan, L. Xi, K. Xia, S. Salahuddin, B. Dieny, and L. You, A spin-orbit-torque memristive device, *Adv. Electron. Mater.* **5**, 1800782 (2019).
- [51] Y. Cao, A. W. Rushforth, Y. Sheng, H. Zheng, and K. Wang, Tuning a binary ferromagnet into a multistate synapse with spin-orbit-torque-induced plasticity, *Adv. Funct. Mater.* **29**, 1808104 (2019).
- [52] A. Kurenkov, S. DuttaGupta, C. Zhang, S. Fukami, Y. Horio, and H. Ohno, Artificial neuron and synapse realized in an antiferromagnet/ferromagnet heterostructure using dynamics of spin-orbit torque switching, *Adv. Mater.* **31**, 1900636 (2019).
- [53] K. Dong, Z. Guo, Y. Jiao, R. Li, C. Sun, Y. Tao, S. Zhang, J. Hong, and L. You, Field-free current-induced switching of L1<sub>0</sub>-FePt using interlayer exchange coupling for neuromorphic computing, *Phys. Rev. Appl.* **19**, 024034 (2023).
- [54] S. Lequeux, J. Sampaio, V. Cros, K. Yakushiji, A. Fukushima, R. Matsumoto, H. Kubota, S. Yuasa, and J. Grollier, A magnetic synapse: multilevel spin-torque memristor with perpendicular anisotropy, *Sci. Rep.* **6**, 31510 (2016).
- [55] B. Zhang, W. Lv, Y. Guo, B. Wang, K. Luo, W. Li, and J. Cao, Realization of multi-level state and artificial synapses function in stacked (Ta/CoFeB/MgO)<sub>N</sub> structures, *Adv. Electron. Mater.* **9**, 2200939 (2023).
- [56] H. Markram, J. Lübke, M. Frotscher, and B. Sakmann, Regulation of synaptic efficacy by coincidence of postsynaptic APs and EPSPs, *Science* **275**, 213 (1997).
- [57] J.-X. Shen, D.-S. Shang, Y.-S. Chai, S.-G. Wang, B.-G. Shen, and Y. Sun, Mimicking synaptic plasticity and neural network using memtransistors, *Adv. Mater.* **30**, 1706717 (2018).
- [58] S. Fukami, J. Ieda, and H. Ohno, Thermal stability of a magnetic domain wall in nanowires, *Phys. Rev. B* **91**, 235401 (2015).
- [59] J. Yun, Y. Sheng, X. Guo, B. Zheng, P. Chen, Y. Cao, Z. Yan, X. He, P. Jin, J. Li, M. Cui, T. Shen, Z. Wang, D. Yang, Y. Zuo, and L. Xi, Tuning the spin-flop transition in perpendicularly magnetized synthetic antiferromagnets by swift heavy Fe ions irradiation, *Phys. Rev. B* **104**, 134416 (2021).
- [60] M. El-Hilo, A. M. de Witte, K. O'Grady, and R. W. Chantrell, The sweep rate dependence of coercivity in recording media, *J. Magn. Magn. Mater.* **117**, L307 (1992).